Electronic Supplementary Material (ESI) for Journal of Materials Chemistry C.

Electronic Supplementary Information

Heterogeneous Modulation of Exciton Emission in Triangular WS_2 Monolayers by Chemical Treatment

Krishna P. Dhakal[§,‡#], Shrawan Roy[#], Seok Joon Yun[§,‡], Ganesh Ghimire[§,‡], Changwon Seo[§,‡], Jeongyong Kim*

[§]Center for Integrated Nanostructure Physics, Institute for Basic Science (IBS), Suwon 16419, Republic of Korea.

[‡]Department of Energy Science, Sungkyunkwan University, Suwon 16419, Republic of Korea.

[#]K. P. D. and S. R. contributed equally to this work.

*Corresponding author: E-mail: j.kim@skku.edu

1. **Schematic of the surface-charge-induced doping effects of TFSI and BV**

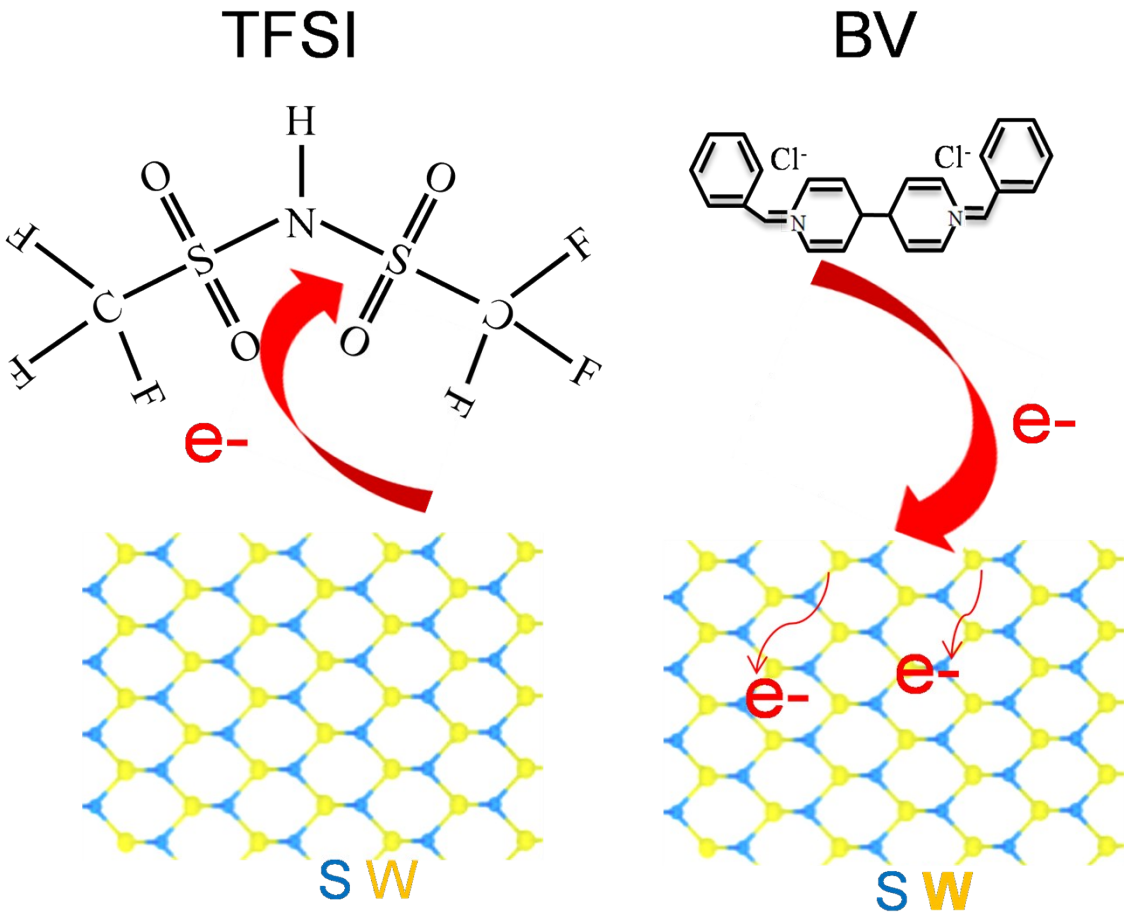

Figure S1: Schematic of the molecular structure of the organic compounds TFSI and BV and two-dimensional lattice structure of the tri-atomic 1L-WS_2 film. Arrows indicate electron withdrawal and donation from and to the 1L-WS_2 films, respectively, by TFSI and BV.

2. TFSI-adsorbed and as-grown 1L-WS_2 film on quartz substrate

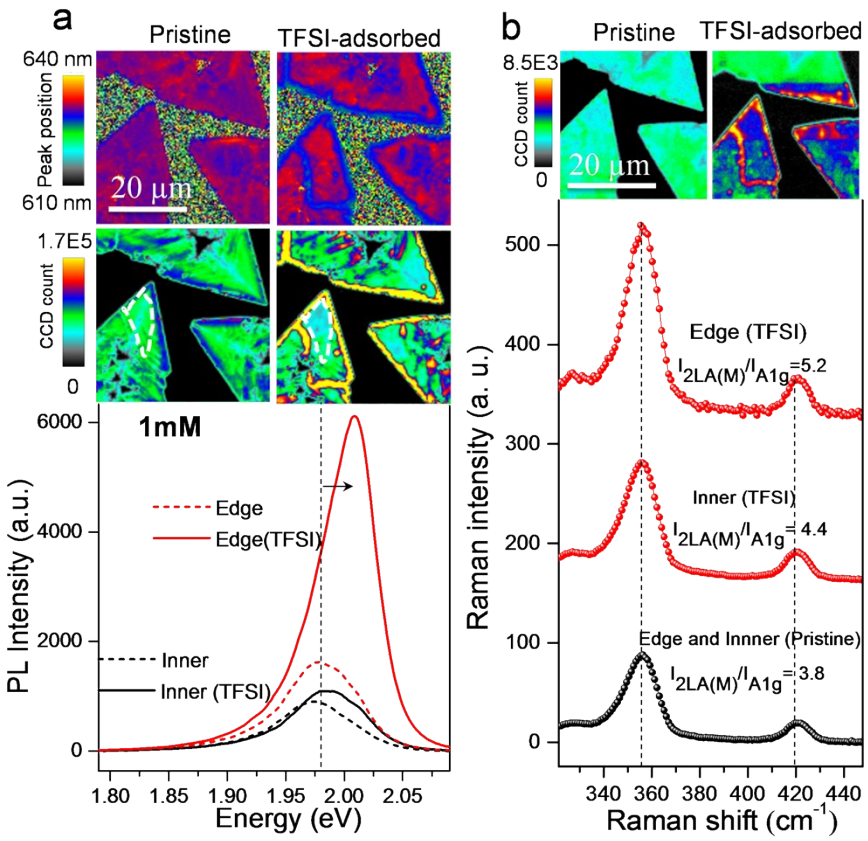

Figure S2: (a) PL spectral images of 1L-WS_2 film grown on quartz substrate before and after adsorption of 1 mM TFSI solution. Upper panel: PL peak position and intensity maps, in which the PL intensity is enhanced and blue-shifted at the edge owing to TFSI adsorption, whereas in the inner region, the changes in the PL intensity and peak position are much smaller. Bottom panel: averaged PL spectra obtained from the edge and inner regions of the 1L-WS_2 before and after TFSI adsorption. (b) Raman spectral maps of 1L-WS_2 film grown on quartz substrate before and after adsorption of 1 mM TFSI solution and averaged Raman spectra from the edge and inner regions showing enhancement of the Raman bands owing to TFSI adsorption. The Raman band intensity of the $E_{2g}{}^1$ mode in the edge region is strongly enhanced compared to that in the inner region, suggesting a large density of passivated defects in the edge region.

3. **Effect of nitromethane solvent used to prepare TFSI solution on the optical properties of the 1L-WS_2 film**

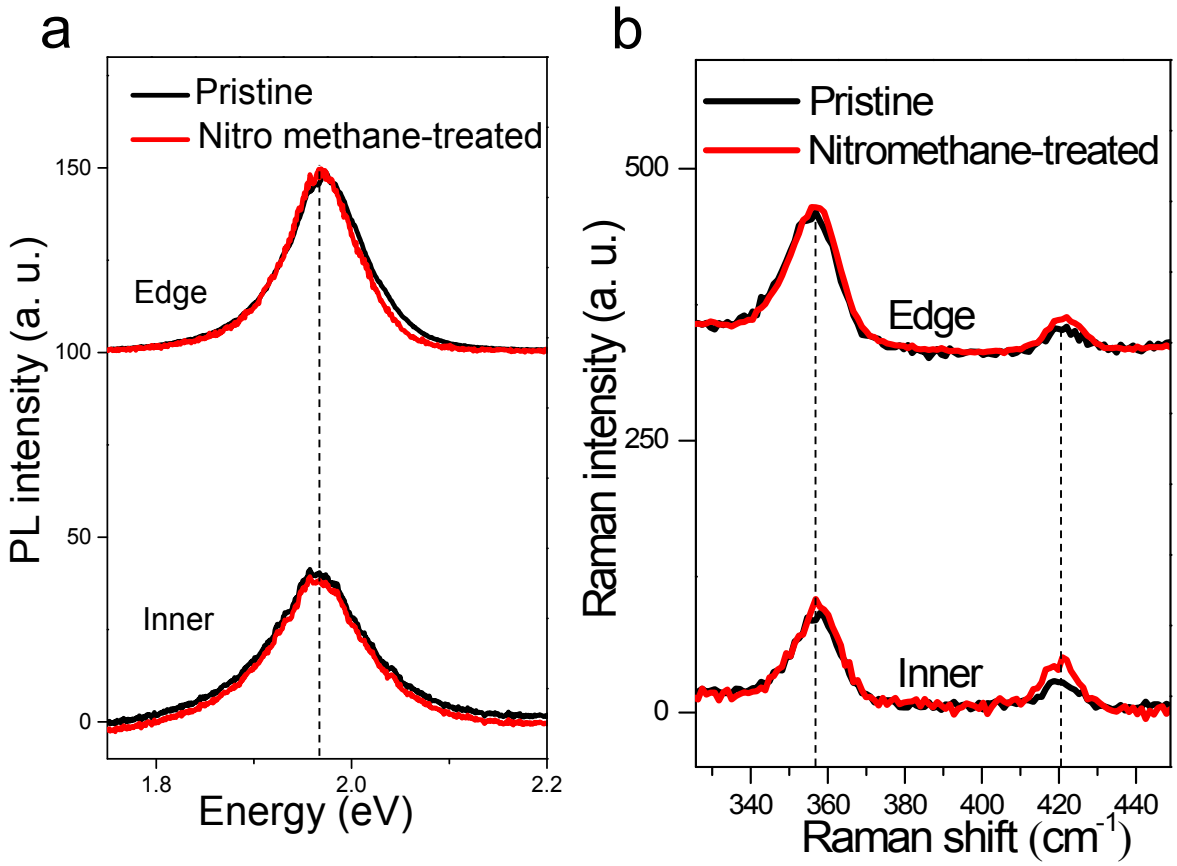

Figure S3: (a) PL and (b) Raman spectra of the edge and inner regions of the 1L-WS_2 film before and after nitromethane treatment. Nitromethane treatment had a negligible effect on the PL and Raman spectra.

4. **Normalized Raman spectra (pristine and after adsorption of 1 mM TFSI)**

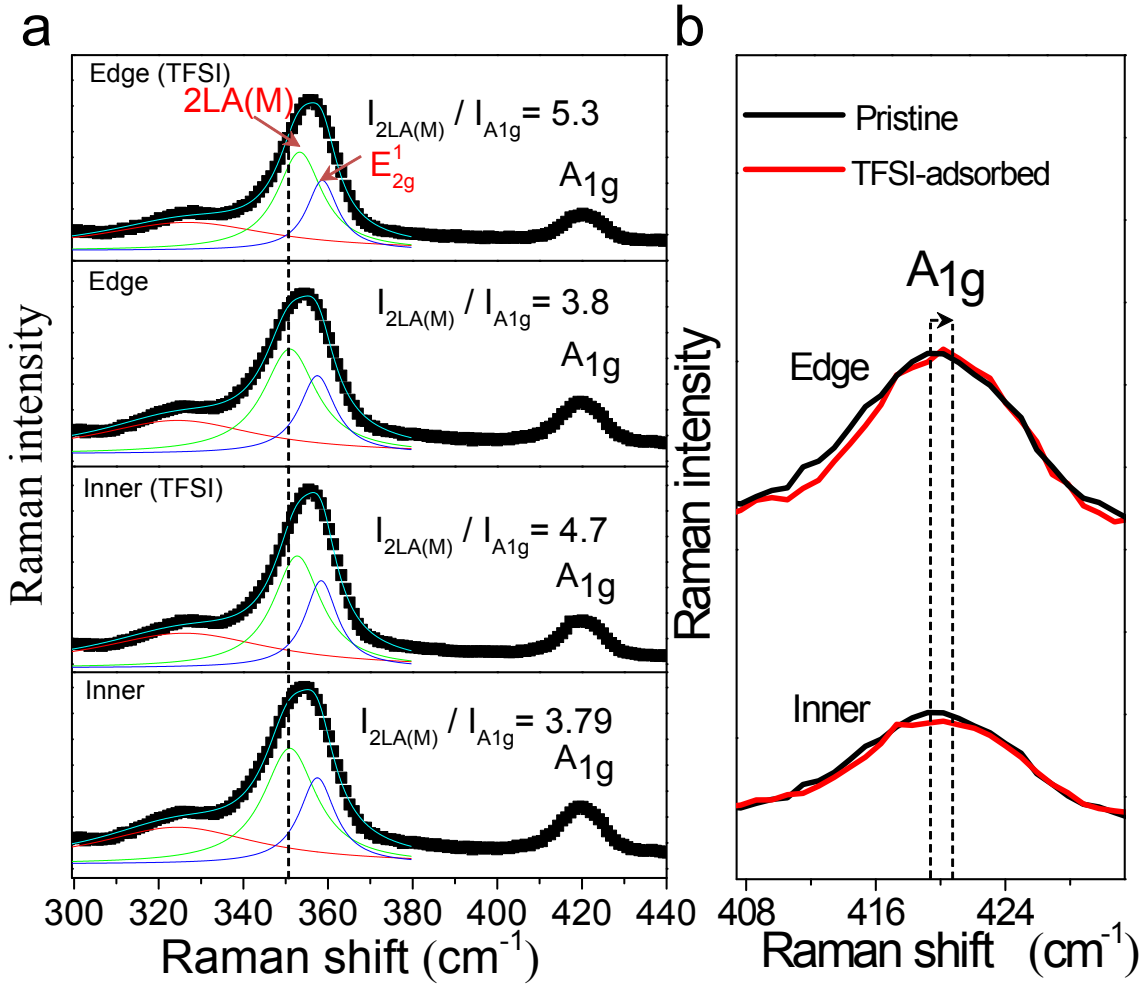

Figure S4: (a) Normalized Raman spectra showing the enhanced 2LA(M) + $E_{2g}{}^1$ Raman band intensity compared to the A_{1g} mode of vibration due to TFSI adsorption. (b) A_{1g} Raman band also demonstrates a small blue-shift due to TFSI adsorption.

5. **Optical characterization of 1L-WS_2 transferred to a cover glass**

5.1 Stepwise cumulative treatments with TFSI solution

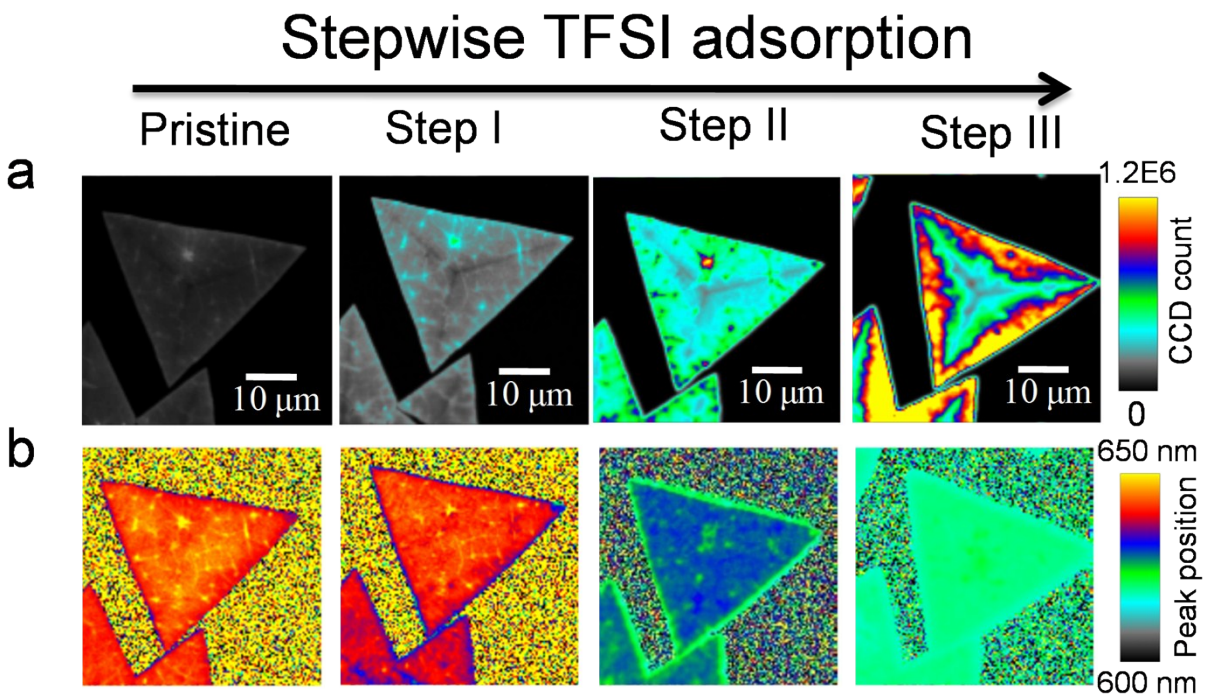

Figure S5: PL (a) intensity and (b) peak position maps during stepwise TFSI application on 1L-WS_2 film.

5.2 Optical absorption spectra of TFSI-adsorbed as-grown 1L-WS_2 flakes on quartz substrate

Optical absorption spectra of the as-grown 1L-WS_2 sample on a quartz substrate before and after TFSI adsorption are shown. Exciton peak A, shown in the inset of Fig. S6, is slightly modified and demonstrates increased absorption near the higher-energy tail of the exciton A band, which may indicate the formation of a large number of neutral excitons.

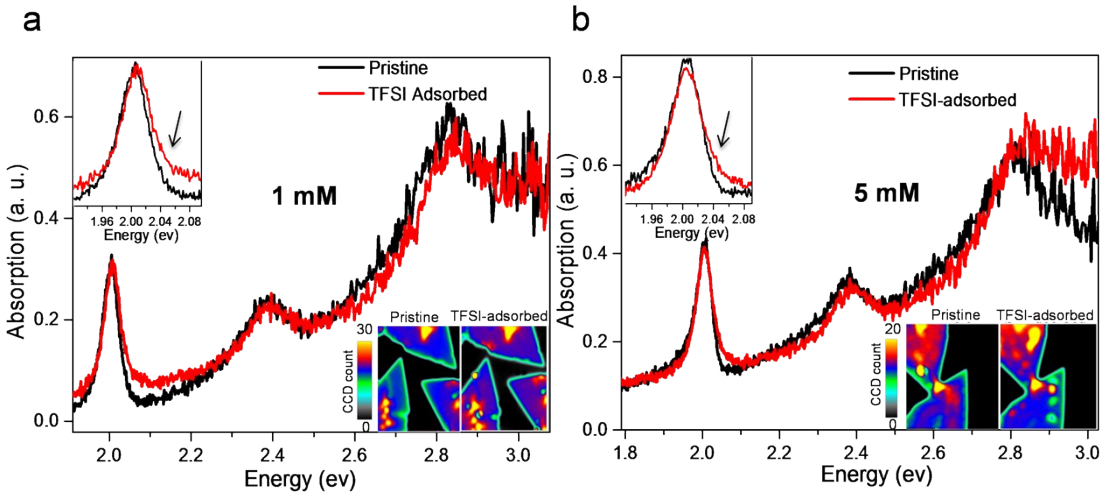

Figure S6: Absorption spectra of pristine 1L-WS_2 before and after adsorption of (a) 1 mM and (b) 5 mM TFSI solution. Insets at lower right show optical absorption spectral maps. The averaged absorption spectra display exciton peaks A, B, and C, where no significant change due to TFSI adsorption was observed. Absorption spectra were obtained by averaging the whole area.

5.3 PL and absorption spectra of 1L-WS_2 before and after transfer to a cover glass with and without TFSI adsorption

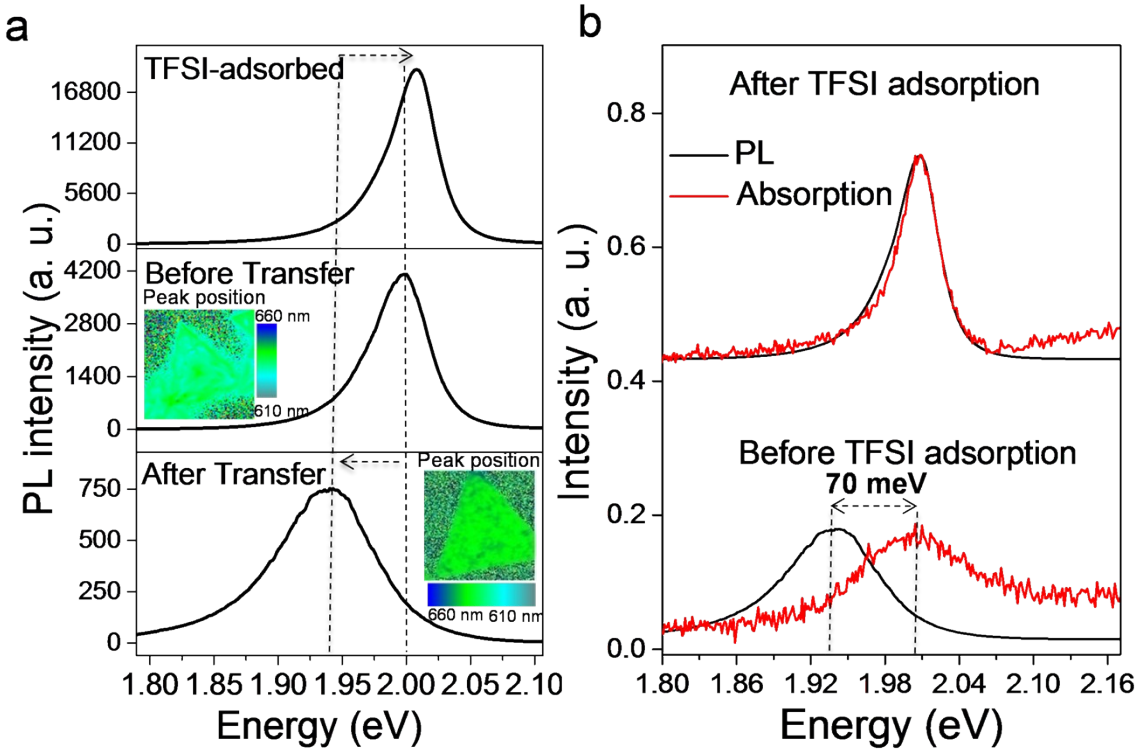

Figure S7: (a) PL spectra of the 1L-WS_2 film as-grown (middle panel), after transfer (bottom panel), and after subsequent TFSI adsorption (top panel). The PL spectral maps are shown as insets. The PL intensity of the 1L-WS_2 film after transfer was lower and red-shifted compared to that of the as-grown sample; further, after TFSI adsorption, the PL peak was greatly enhanced, narrower, and blue-shifted compared to that of the as-grown sample. (b) PL and absorption peak positions of 1L-WS_2 before and after TFSI adsorption. A 70 meV Stoke shift was initially observed between the absorption and PL spectra, but after TFSI adsorption, both the PL and absorption spectra overlap perfectly, showing the same peak position and shape. PL and absorption spectra were obtained by averaging whole area.

6. Power-dependent PL of 1L-WS_2 film before and after TFSI adsorption

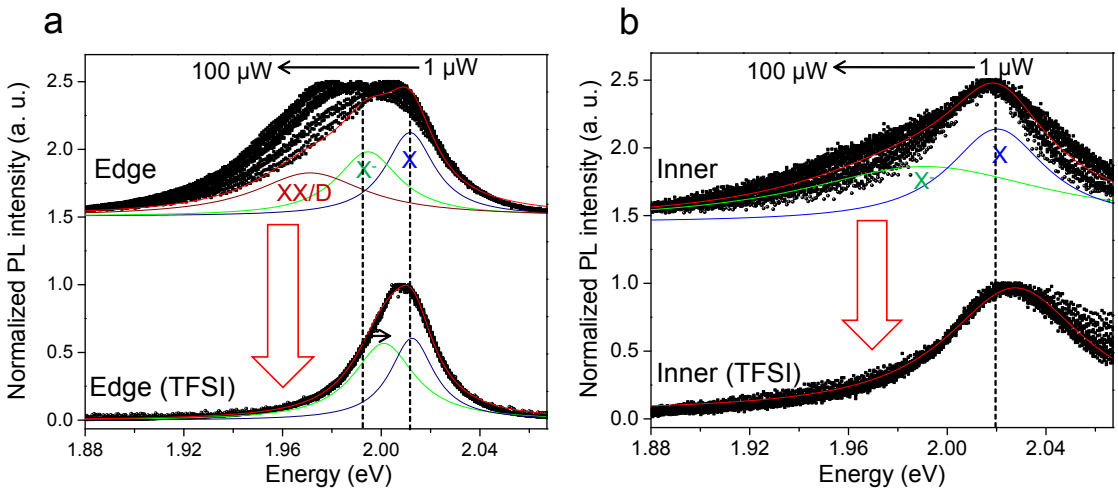

Figure S8: Laser-power-dependent PL spectra obtained in the (a) edge and (b) inner regions of 1L-WS_2 before and after TFSI adsorption. Interestingly, TFSI treatment reduced the FWHM of the PL spectra, suggesting dominant X and X^- recombination and reduced PL originating from XX/D recombination. The reduced FWHM is consistently observed at the edge and in the inner region owing to TFSI adsorption.

7. PL, Raman, and absorption spectra of 1L-WS_2 film before and after adsorption of 5 mM BV solution

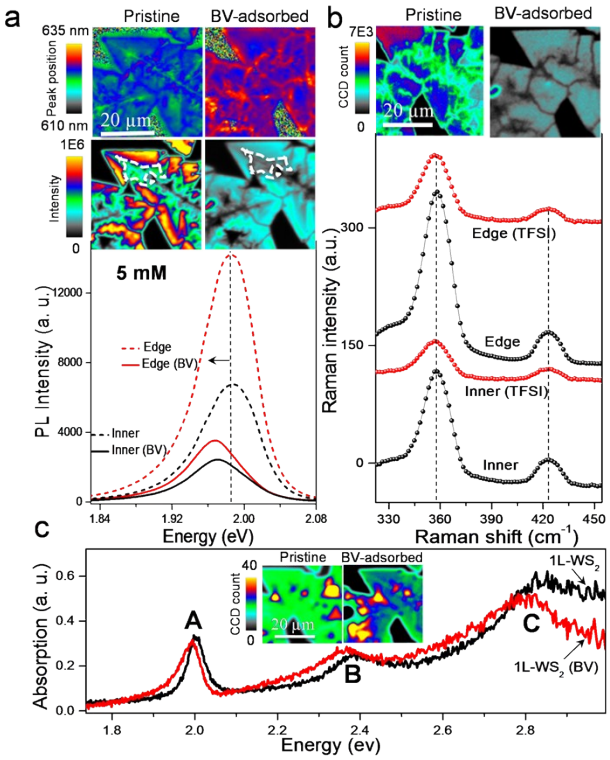

Figure S9: (a) PL peak position and intensity spectral maps and average PL spectra obtained from the edge and inner regions of 1L-WS_2 grown on a quartz substrate before and after adsorption of 5 mM BV solution. PL spectra and PL images both reveal reduced PL intensity and a red-shift of the PL peak due to BV adsorption. (b) Raman spectral maps and averaged Raman spectra obtained from the edge and inner regions show reduced Raman band intensity due to BV adsorption. The Raman band intensity of the E_{2g}^1 mode was more strongly reduced in the edge region than in the inner region. (c) Optical absorption spectra of pristine and BV-adsorbed 1L-WS_2. Absorption peaks A, B, and C are observed, where exciton peak A is red-shifted and its intensity is reduced by BV adsorption. Inset shows optical absorption spectral maps of 1L-WS_2 obtained before and after BV adsorption.

8. Comparison of PL spectra of 1L-WS_2 sample grown on Si/SiO_2 substrate before and after adsorption of 5 mM BV solution

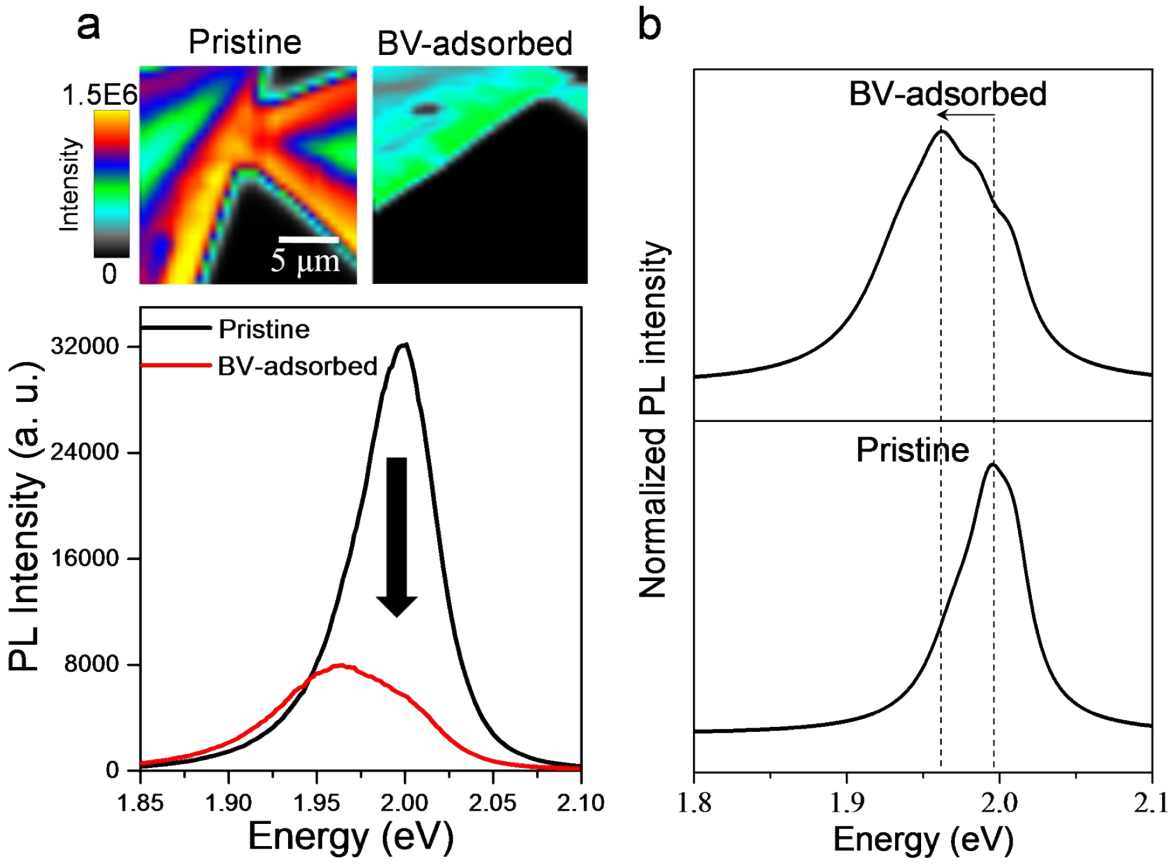

Figure S10: (a) PL intensity maps and averaged PL spectra obtained by averaging whole area. of 1L-WS_2 grown on Si/SiO_2 substrate obtained before and after adsorption of 5 mM BV solution. PL images and PL spectra both reveal reduced PL intensity and broadening and a red-shift of the PL peak due to BV adsorption. (b) Normalized PL spectra showing the reduction and red-shift of PL intensity after adsorption of BV. The PL spectral modification of the sample grown on the Si/SiO_2 substrate with BV adsorption was similar to that of the as-grown sample on the quartz substrate.

9. Laser-power-dependent PL analysis before and after BV adsorption of 1L-WS_2 film

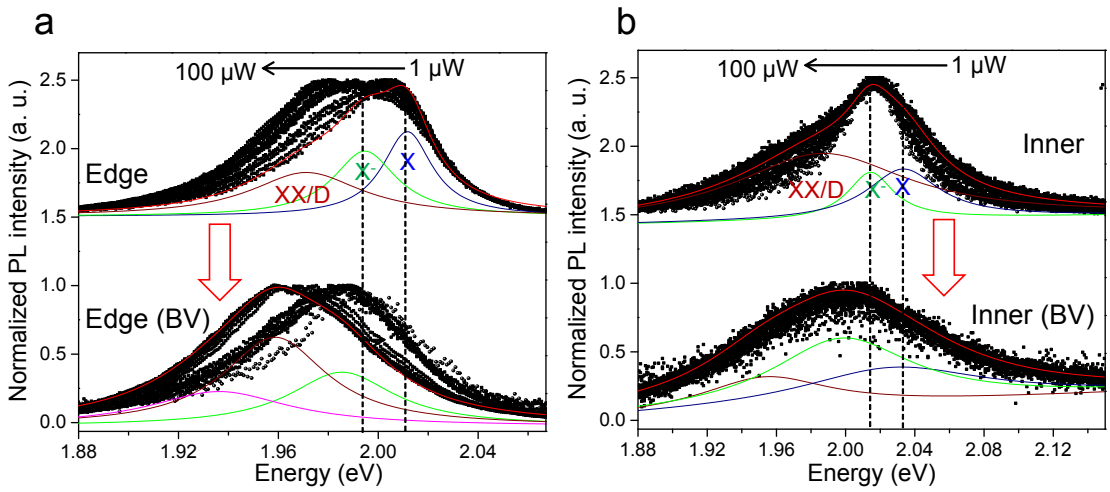

Figure S11: Laser-power-dependent PL spectra of the (a) edge and (b) inner regions of 1L-WS_2 before and after BV adsorption. The peak is red-shifted by the n-doping effect of BV.

10. Normalized Raman spectra of 1L-WS_2 before and after adsorption of 1 mM BV

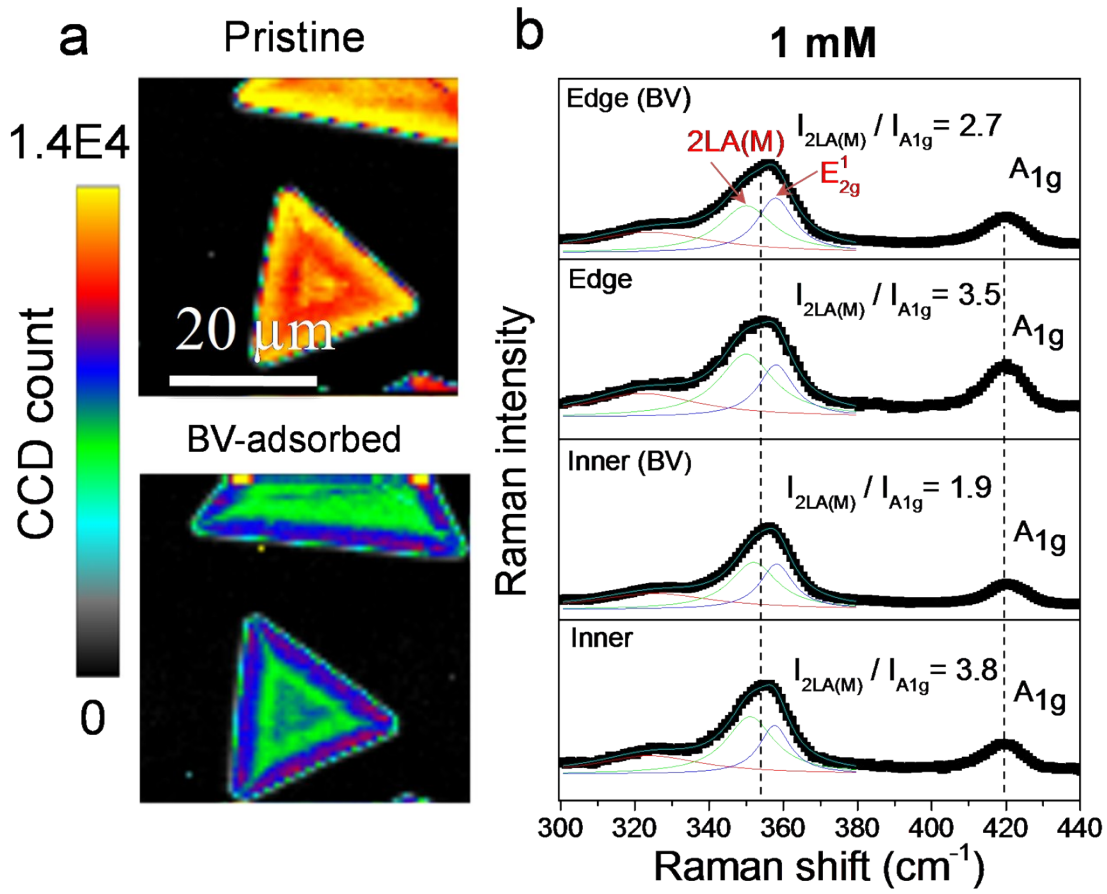

Figure S12: (a) Raman intensity maps and (b) normalized Raman spectra of 1L-WS_2 before and after BV adsorption. The A_{1g} mode intensity was enhanced by BV adsorption.

11. Effect of the toluene solvent used to prepare the BV solution on the optical properties of the 1L-WS_2 film

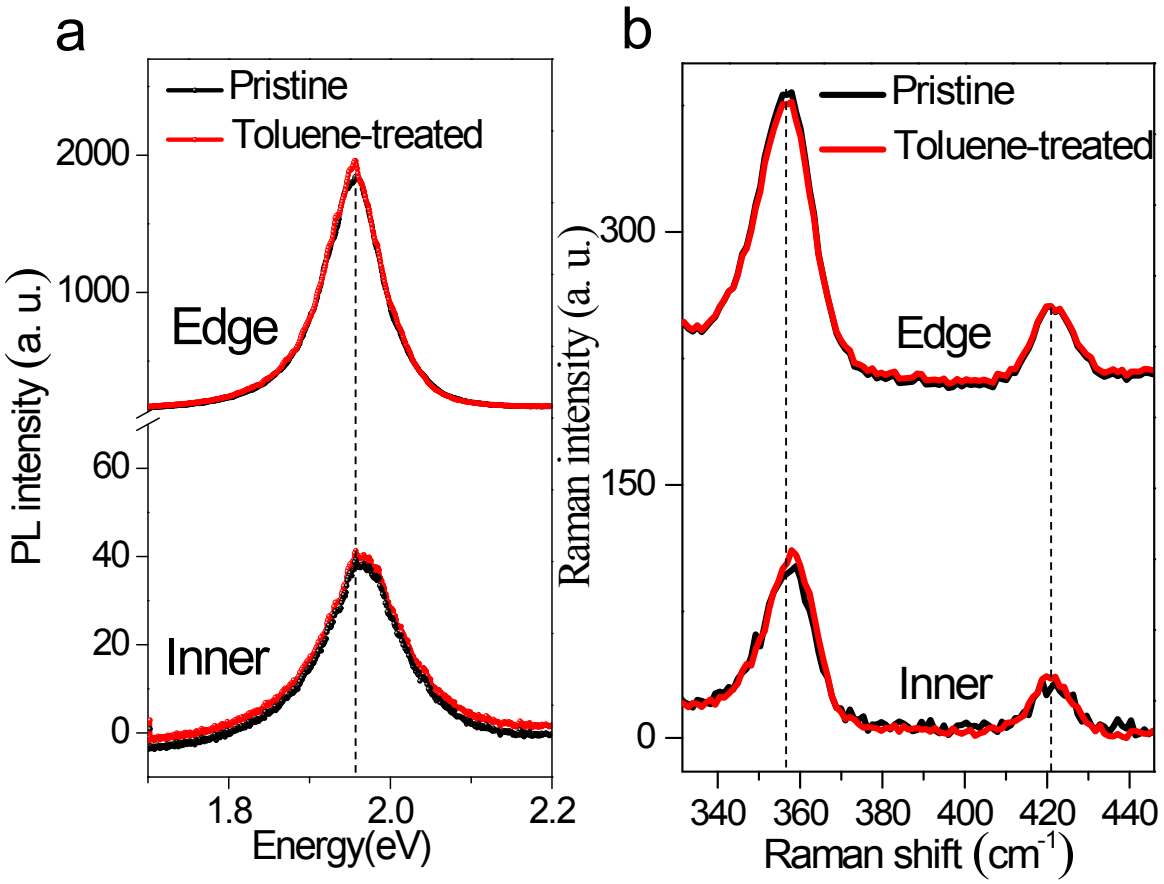

Figure S13: (a) PL and (b) Raman spectra of the edge and inner regions of 1L-WS_2 before and after toluene treatment. Toluene treatment had a negligible effect on the spectra.

12. Comparison of absorption spectra with and without TFSI and BV adsorption on 1L-WS_2 film

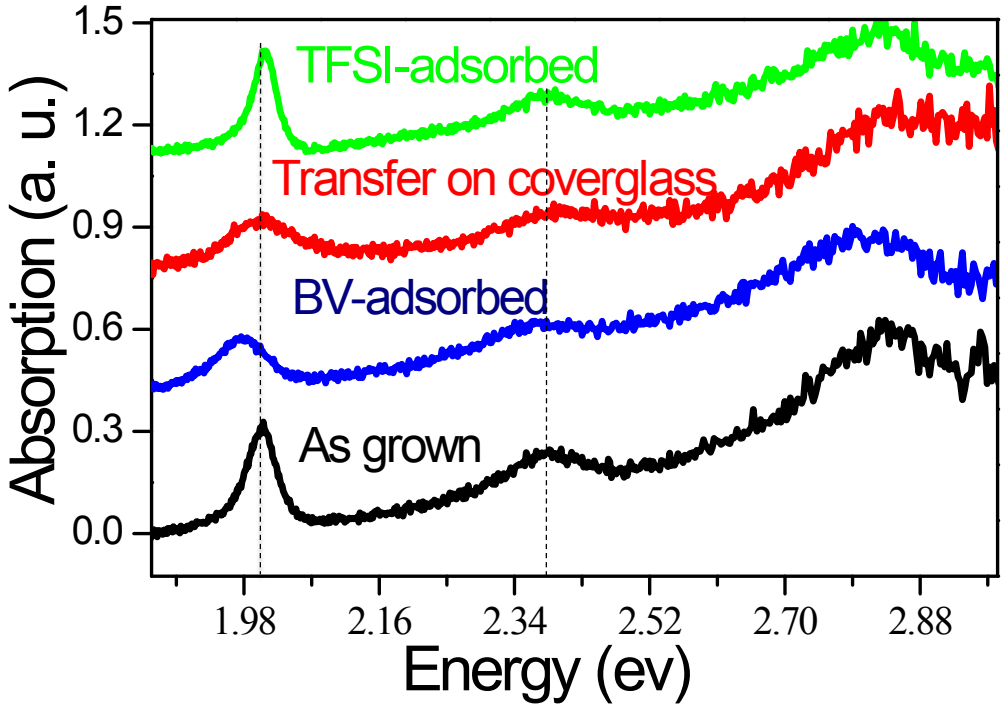

Figure S14: Absorption spectra obtained by averaging whole area of 1L-WS_2 before (grown on quartz substrate and transferred to glass substrate) and after chemical adsorption of TFSI and BV. The peak position and shape of the absorption spectra of 1L-WS_2 with and without TFSI and BV adsorption are compared. The absorption peak position is slightly blue-shifted after TFSI adsorption and red-shifted after BV adsorption compared to that of the as-grown sample.